Electronic Supplementary Information

A "Turn-On" Silver Nanoclusters Based Label-Free Fluorescent Sensor for Folate Receptor Detection and Its Application on Cancer Cells Imaging under Visual Analysis

Hong Jiang,[a #] Gang Xu,[a #] Baojuan Wang,[b] Xiaojun Zhang,[a] Guangfeng Wang[a,c*]

[a] *Key Laboratory of Chem–Biosensing, Anhui province; Key Laboratory of Functional Molecular Solids, Anhui province; College of Chemistry and Materials Science, Anhui Normal University, Wuhu, 241000, P R China*

[b] *College of Life and Science, Anhui Normal University, Wuhu, 241000, P R China*

[c] *State Key Laboratory of Chemo/Biosensing and Chemometrics, Hunan University, Changsha, 410082, P R China*

E-mail: xjzhang@mail.ahnu.edu.cn; wangyuz@mail.ahnu.edu.cn

 # Hong Jiang and # Gang Xu are co-first authors and contributed equally.

*Corresponding author: E-mail: wanglun@mail.ahnu.edu.cn; Fax: +86-553-3869303; Tel: +86-553-3869303

1 Experimental section.

Reagents and Chemicals. HPLC-purified oligonucleotides with specific sequences were obtained from Sangon Biotechnology Co. Ltd. (Shanghai, China) and the sequences used in assays are as follows:

S1: 5'-TATTACTTACTTACTTACTT-NH_2-3'

S2: 5'-CCCCCCCCCCCCCAAGTAAGTAAGTAAGTAATA-3'

SWCNTs (single-walled carbon nanotubes, diameter ≤ 5 nm, and lengths 5-15 μm) were also purchased from Sangon Biotechnology Co. Ltd. (Shanghai, China). The morphology of the SWCNTs is characterized by scanning electron microscopy (SEM) in Fig. S2. Phosphate-buffered saline (PBS, pH=7.4, 10 mM if not illustrated), 1-ethyl-3-(3-dimethyl-aminopropyl) carbodiimide hydrochloride (EDC), N-hydroxysulf-osuccinimide (sulfo-NHS), Tris-(hydroxymethyl) aminomethane (Tris) and N,N-Dimethylformamide (DMF) were obtained from the Sinopharm Chemical Reagent Co. Ltd. (Shanghai, China). Bovine hemoglobin (BHb), Goat-anti-human IgG, Chronic viral hepatitis (CVH), Bovine serum albumin (BSA), Exonuclease I (Exo I), Folate receptor 2 human (FR) and Folic acid (FA), trypsin was purchased from Sigma Aldrich Chemical Co. Ltd. (USA). All chemicals were of analytical grade or better and were used without further purification. Ultrapure water was used throughout all experiments.

Apparatus. Fluorescence spectra were recorded on F-4500 FL Spectrophotometer (Hitachi, Japan) equipped with a quartz cell (1cm×1cm) in the fluorescence mode. Fluorescence intensity was recorded at 620 nm with an excitation wavelength of 568 nm (if no special description). Ultraviolet-visible absorption spectra were measured on UV-3010 spectrophotometer (Hitachi, Japan). Fourier Transform Infrared Spectroscopy (FTIR) were measured using an FTIR-8400S spectrometer (Japan, Shimadzu) in 500-4000 cm^{-1} region using powdered sample on a KBr plate. Scanning electron microscopy (SEM) images of the prepared composites were obtained using Hitachi S-4800 SEM (operated at 10 kV). High-resolution transmission electron microscope (HRTEM) observations for the morphological measurements of AgNCs-S2 were performed on JEOL-2010F with an acceleration voltage of 200 KV. Decay curves measurements were performed with the time correlated single photo counting technique on the combined steady state and lifetime spectrometer (Edinburgh Analytical Instruments, FLS920). Ultrapure water was obtained through PSDK2-10-C (Beijing, China). All electrochemical measurements were performed using a CHI 660B (Shanghai Chen Hua Instrument Co. Ltd.) electrochemical workstation in a conventional three-electrode system with glassy carbon electrode (GCE) as working electrodes, a saturated calomel electrode (SCE) as reference electrode and the platinum foil electrode as counter electrode. All pH measurements were measured with a Model pHs-3c meter (Shanghai, China). All optical measurements were performed with slit information that Ex slit=2.5 nm, Em slit=5.0 nm at room temperature under ambient conditions. Confocal laser scanning microscopy characterization was conducted by a confocal laser scanning biological microscope (FV1000-IX81, Olympus, Japan) with FV5-LAMAR for excitation at 568 nm and a variable band pass emission filter set to 600-700 nm. Fluorescence micrographs were recorded with a Zeiss Apotome inverted microscope combined with a 100x oil immersion objective. Flow cytometric assay was performed using Cytomics FC500 Flow Cytometry (Beckman Coulter Ltd.).

Preparation of FA-linked S1 (FA-S1) and FA/FR-linked S1 (FR/FA-S1). FA was conjugated to the 3'-NH_2 of the S1 with the succinimide coupling (1-ethyl-3-(3-dimethyl-aminopropyl) carbodiimide hydrochloride/ N-hydroxysuccinimide (EDC-NHS)) method.[1] First, 0.5 mL of 20 mM S1 was mixed

with 0.5 mL of 100 mM Tris-HCl (pH 7.4) (including 10 mM FA, 1 mM EDC, and 5 mM sulfo-NHS), and then incubated in dark for 3 h at 37 °C. The obtained FA-S1 solution was dialyzed against phosphate buffer solution (PBS) using a membrane with molecular weight cutoff of 1000 Da to remove the excessive folate acid. Afterwards, to fabricate FA-S1 with different concentrations of FR (FR/FA-S1), a series of varying concentrations of FR were joined into the preceding solutions entirely for sufficiently incubating at 37 °C for 2 h in dark. The FTIR spectroscopy was studied to confirm successful synthesis of FA-S1 (Figure S1A). The peak at 1651 cm^{-1} in curve a was attributed to N-H bending vibrations of the ssDNA modified with $-NH_2$. The peak at 1697 cm^{-1} in curve b was attributed to C=O stretching vibrations in the carboxylic groups of FA. However, with the sample of FA-S1, both the peak at 1624 and 1674 cm^{-1} could be observed as curve c shows. It can verify the successful conjugation of FA with S1. In addition, after its conjugation with S1, the UV absorption at 360 nm for FA is blue-shifted to 330 nm (Figure S1B) and the fluorescent emission peak at 469 nm for FA moves to 447 nm (Figure S1C). Fig. S1D shows that after dialysis to remove the free FA, the color of FA-S1 solution become transparent compared with the original yellow color of FA solution before conjugation with S1. These significant differences further proved the successful synthesis of FA-S1.

Synthesis of oligonucleotide-stabilized Ag nanoclusters (AgNCs-S2) and its electrochemical characterization. The oligonucleotide-stabilized Ag nanoclusters were synthesized according to previous reports.[2] Briefly, $AgNO_3$ in a molar ratio of 6 : 1 was added to a 10 mM S2 solution (60 μL, dissolved in PBS) followed by the vigorous shaking of the solution for 30 sec. After stirring, freshly prepared $NaBH_4$ (10 μL) with the same concentration (60 mM) was added into this mixture (80 μL) for reduction followed by vigorous shaking of the mixture for 30 sec and the reduced oligonucleotide-Ag solution was incubated at 4 °C and allowed to react for 1 h in the dark. Silver ions bound with cytosine[3] were reduced to form nanoclusters. AgNCs-S2 was synthesized and would be utilized for further fluorescence detection. To verify whether AgNCs-S2 was synthesized successfully as we designed, electrochemical characterization was processed. 20 μL AgNCs-S2 (10 μM) were dropped onto the cleaned GCE and dried for about 6 h at room temperature naturally for the cyclic voltammetry (CV) study. The CV measurement from -500 mV to 600 mV (vs. SCE, scan rate: 50 mV/s) was carried out in PBS.

Preparation of AgNCs-S2/SWCNTs. The purified SWCNTs were sonicated in N,N-Dimethylformamide (DMF) solution for 1 h until forming a homogeneous black solution. To fabricate AgNCs-S2/SWCNTs structure, 100 μL PBS buffer containing 20 μL SWCNTs (1 μM) and the aforementioned AgNCs-S2 (10 μM) was allowed to incubate for 30 min at room temperature in dark environment. Then the resulting solution consisting of AgNCs-S2/SWCNTs was used directly for FR detection.

Cell culture and cell imaging. The HeLa (human cervical cancer) of cervix cell line CCL-2 and human umbilical vein endothelial cells (HUVEC) were obtained from the American Type Culture Collection. HeLa cells were cultured in Corning-culture dishes in Dulbecco's modified eagle medium (DMEM) at 37 °C and 5% CO_2 atmosphere, supplemented with a 10% heat-inactivated fetal bovine serum. The cells grown on glass-bottom culture dishes containing 0.4 mL of culture medium were first

incubated with 400 μL mixture containing 10 μM FA-S1, 10 μM AgNCs-S2, and 1 μM SWCNTs for 3 h at 25 °C. Further 110 U Exo I was added into the mixture. Competition experiments were also conducted where the cell culturing was pre-treated with saturated FA solution for 1.0 h prior to FA-S1 treatment. Furthermore, control experiments using normal cells were carried out using the same procedure. Their fluorescence images were taken by depositing 30 μL of the incubated suspensions onto a thin clean glass above a 40×4 objective on the confocal microscope after being washed with PBS twice to ensure no dead cells and dissociative FA were left.

Cellular binding and internalization in Hela cells were also examined. For the binding analysis, $\mathbf{10^6}$ cells (Hela or HUVEC cells) were incubated with FA-S1, AgNCs-S2, Exo I and SWCNTs (nanocomplexes) or S1, AgNCs-S2, Exo I and SWCNTs (free FA nanocomplexes) for 3 h and in 200 μL of cell media for 2 h at 37 ^{o}C. Then cells were centrifuged, washed twice with 400 μL of PBS, and finally resuspended in 400 μL of PBS for flow cytometirc analysis on the flow cytometer. For the internalization assay, cells were treated with trypsin for 5 min and the same process was then performed.

For the endocytosis pathways analysis, Hela cells were seeded in 6-well plates ($\mathbf{10^6}$ cells per well) and cultured for 48 h. Afterwards, the cells were pre-incubated with several inhibitors specific for different endocytosis pathways [4] [chlorpromazine (CPZ, 10 μM) for clathrin-mediated endocytosis; nystatin (NYS, 25 μg/mL) for cavelolin-mediated endocytosis; amiloride (AMI, 1 mM) for macropinocytosis; methyl-β-cyclodextrin (MCD, 3 mM) for lipid raft] for 1 h at 37 °C, respectively. Then the cells were incubated with nanocomplexes in the presence of the inhibitors for another 3 h. After washing the cells by 4 °C PBS twice, the cells were lysed with Pierce IP lysis buffer (Thermo Scientific) and centrifuged. Fluorescence of AgNC in the supernatant were measured.

Quantitative analysis of FR with AgNCs-S2/SWCNTs. 110 Units Exo I was added into 100 μL FA-S1 solution containing various concentration of FR. Followed by incubation, the redundant FA-S1 was digested into fragment, for 20 min at 25 °C. After the digestion, solutions containing various concentrations of FR/FA-S1 were heated to 80 °C for 10 min to inactivate the Exo I, and then mixed with 100 μL pre-prepared AgNCs-S2/SWCNTs after slowly equilibrate to the room temperature. The resultant mixture was incubated at room temperature for detection processes containing investigation of kinetic behaviors. Then the polydispersed nanomaterials were filtered using filter film (the pore size: <0.22μm), followed by the fluorescent measurement of solution containing various concentration of FR. Additionally, to study the role of cancer cells, SWCNTs and Exo I, respectively, control experiments were carried on. The detection process was all the same with the above except the addition of FR, SWCNTs or Exo I, respectively. In order to detect the cancer cells, HeLa cells were trysinized in the presence of 0.25% trypsin solution and collected from the medium by centrifugation at 3000 rpm for 5 min. The collected cells were washed with saline twice and resuspended in saline to achieve the desired concentration. The process is similar to the above steps and then the resulted product for fluorescent measurement.

2 The characterizations of FA-S1 and SWCNTs.

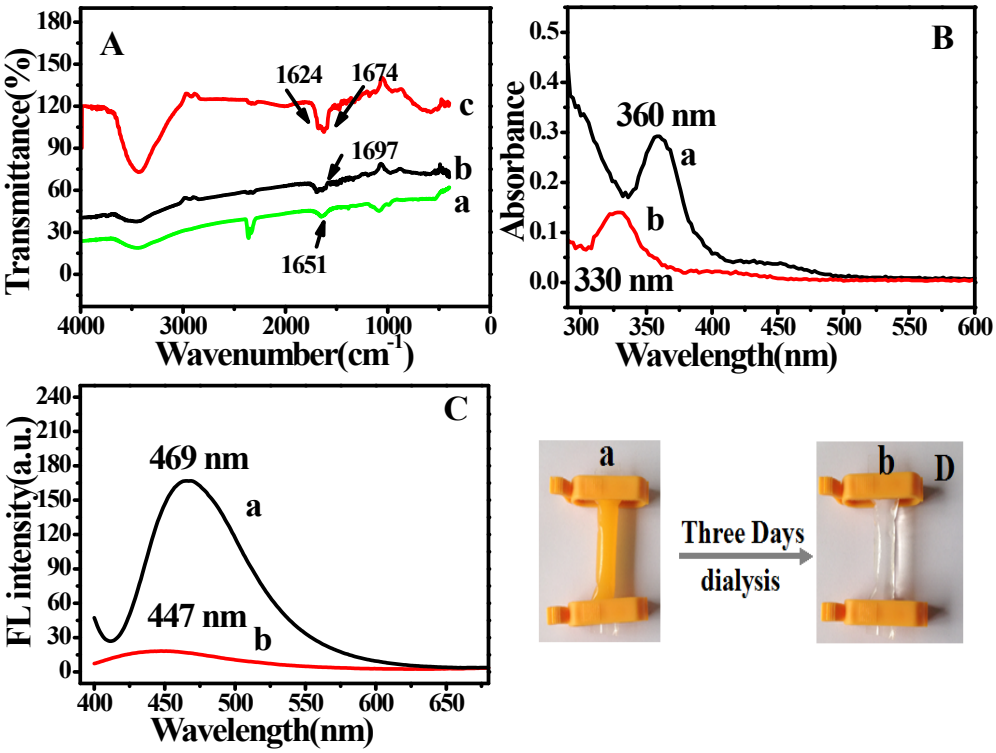

Fig. S1 (A) Fourier transformed-IR spectra of S1 (a), FA (b) and FA-S1 (c). (B) UV-vis absorption of FA (black) and FA-S1 (red). (C) Fluorescence emission spectra of of FA (black) and FA-S1 (red). (D) Photographs of FA-S1 solution before (a) and after (b) dialyzation against PBS using a membrane with molecular weight cutoff of 1000 Da.

Fig. S2 SEM image of the single-wall carbon nanotubes (SWCNTs) sample used in this work.

3 The characterizations of AgNCs-S2.

As shown in Fig. S3A, the fluorescent AgNCs (5 μM) stabilized by the chosen oligonucleotide S2 presented a series of distinctive fluorescence emission peaks at 580 nm, 601 nm, 620 nm, 639 nm and 660 nm with the variation of excitation wavelengths. The maximum excitation and emissions wavelengths of the as-prepared fluorescent AgNCs-S2 were 568 nm and 620 nm, respectively, as shown in Fig. S3B. The maximum fluorescence spectra information was utilized in the following experiment to evaluate the effect of different analytes on the fluorescence emission of AgNCs-S2. Fig. S3C shows the fluorescence decay dynamics of AgNCs-S2 and the results show that the lifetime of the AgNCs-S2 was active. Furthermore, the fluorescence intensity of AgNCs-S2 as a function of time was studied to search the ideal time for detection. As Fig. S3D showed, the fluorescence can keep the highest intensity for about 6 h and decreased a lot after that, so we needed to control the total time (incubation and reaction) within 6 h which was long enough. High resolution transmission electron microscopy (HRTEM) images (Inset) demonstrated that the diameters of AgNCs were mainly distributed in the range of 1-3 nm with average diameter of 2 nm.

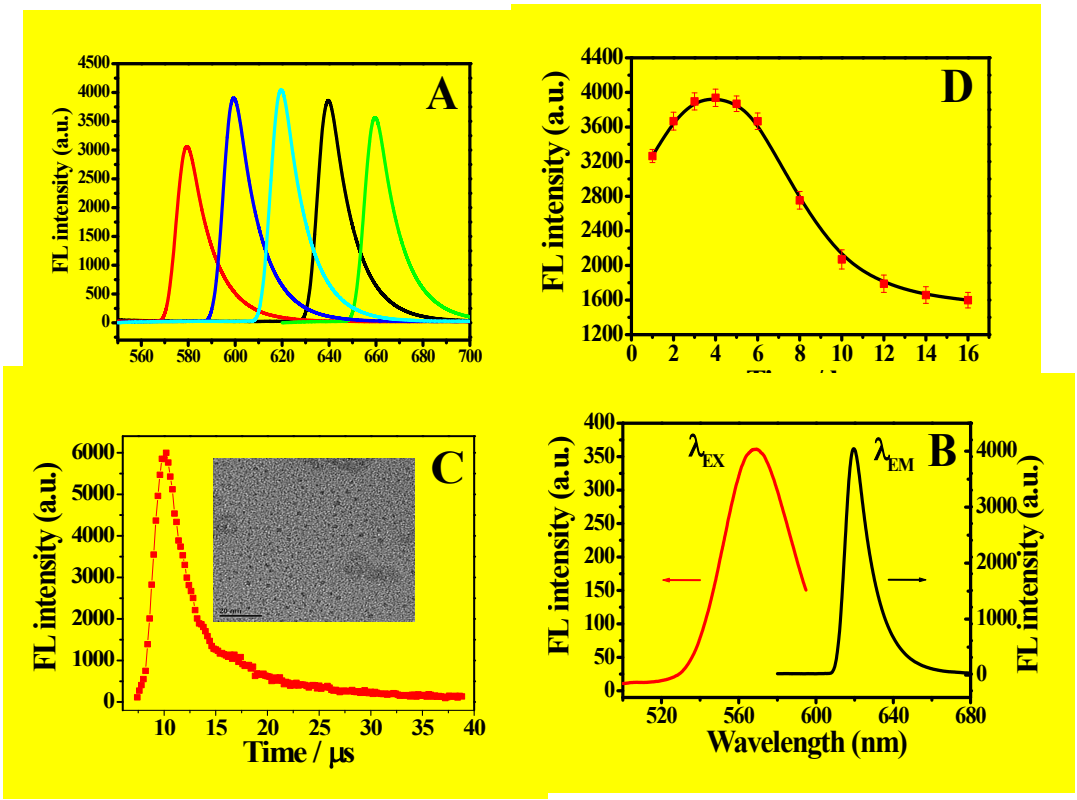

Fig. S3 (A) Fluorescence emission spectra of obtained AgNCs-S2 under different excitation wavelengths. (B) Fluorescence emission spectra of obtained AgNCs-S2 under maximum fluorescence excitation and emission spectra information. (C) Fluorescence decay of AgNCs-S2. Inset: HRTEM image of the signal-templated AgNCs. Scale bar is 20 nm. (D) Time revolution of the fluorescence intensity of AgNCs-S2. Fluorescence intensity was recorded at 620 nm with an excitation wavelength of 568 nm.

4 The FRET effect between AgNCs-S2 and SWCNTs.

The FRET effect between AgNCs-S2 and SWCNTs is the most important section of our detection proposal. To evaluate the efficiency, we processed assays and their details are as below. Fig. S4A depicts the alteration of absorption responses of 10 μM AgNCs-S2 towards SWCNTs addition. The

corresponding absorption intensity at 510 nm increased dramatically and there was a slight red-shift phenomenon after the addition of 20 μL SWCNTs. As shown in Fig. S4B, the fluorescence intensity of AgNCs-S2 at 610 nm decreased significantly after the addition of SWCNTs. The change of both absorption and fluorescence spectrum are consistent with the previous report.[5] The possible explanation is the occurrence of FRET between AgNCs-S2 and SWCNTs. Because of the formation of the π-π stacking interactions between aromatic nucleotide bases and SWCNTs with sp^2 electronic hybrid structure and a large conjugate plane, it results in the twining of AgNCs-S2 around SWCNTs, in which case the AgNCs-S2 and SWCNTs were taken into close proximity which made the occurrence of FRET.

What's more, the electrochemical property of AgNCs in the absence and presence of SWCNTs was also investigated. Fig. S4C shows an oxidation peak at 0.37 V vs. SCE in cyclic voltammetry (CV),[6] and nearly decreases to a steady state by the addition of SWCNTs, we concluded that AgNCs-S2 were formed in C-rich S2 successfully and there was FRET process between AgNCs-S2 and SWCNTs when SWCNTs added. All results reveal that SWCNTs can efficiently quench the fluorescent of AgNCs-S2 originated from the intertwining of fluorescent AgNCs-S2 on SWCNTs, which leads to electron or energy transfer.[7]

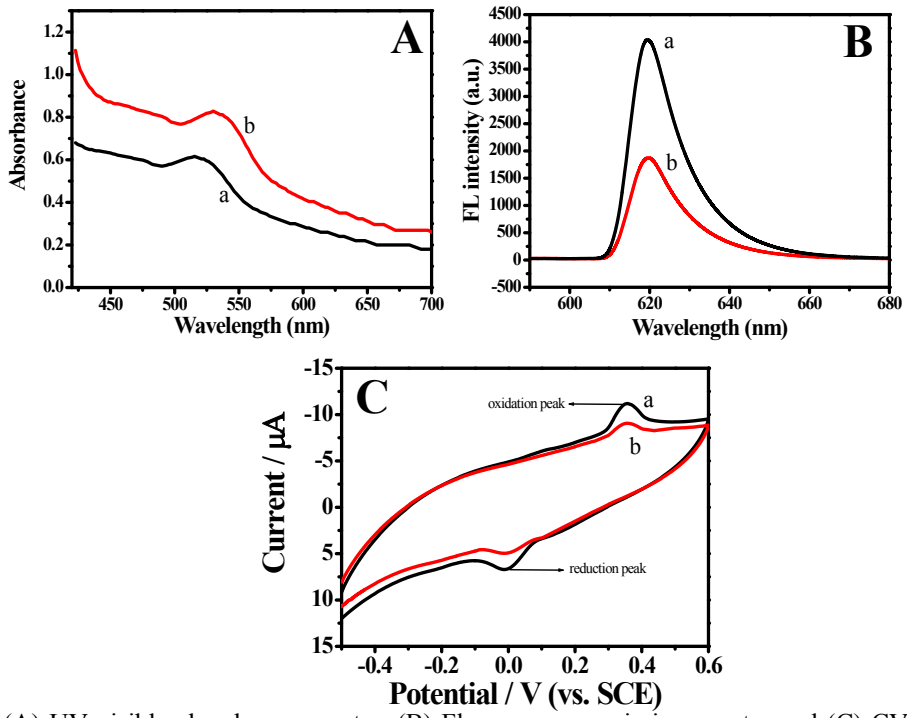

Fig. S4 (A) UV-visible absorbance spectra, (B) Fluorescence emission spectra and (C) CV in PBS at the san rate of 50 mV/s of AgNCs-S2 (curve a) and AgNCs-S2/SWCNTs (curve b). Fluorescence intensity was recorded at 620 nm with an excitation wavelength of 568 nm.

5 Feasibility investigation of the proposed fluorescent sensor.

Feasibility investigation of this assay for the detection of FR activity was proceeded. The fluorescent response of solutions containing different concentrations of FR was studied. As shown in Fig. S5, compared curve e with curve a, the fluorescence intensity of AgNCs-S2 decreased dramatically with the addition of SWCNTs due to FRET effect. The intensity increased significantly in this condition

which containing AgNCs-S2, FA-S1, SWCNTs which is shown in curve d. The possible reason can be ascribed to the hybridization between S1 and S2, resulting in the desorbing of AgNCs-S2 from SWCNTs surface and disturbing the FRET event. In order to confirm the effect of Exo I in the proposed biosensor proposal, curve b showed that in the presence of Exo I, the fluorescence enhancement disappeared because of the digestion of S1 by Exo I. According to the terminal protection mechanism, we have designed FR-FA modified S1 substituted for S1 in the presence of Exo I. Curve c described the detailed information about this process, Curve c showed that the fluorescence enhancement reappeared when the reaction solution containing AgNCs-S2, FA-S1, SWCNTs, Exo I, FR. The enhancement was ascribed to the formation of the duplex DNA between S1 and S2. In this biosensor proposal, with the good affinity between FA and FR, the FA-S1 was bound with FR macromolecules which may convey a steric hindrance, preventing Exo I from approaching and cleaving the phosphodiester bond adjacent to the 3' end of S1 which made S1 not be degraded by Exo I.[8] All assays proved the proposal that AgNCs-S2/SWCNTs can only reflect fluorescence in the presence of FR in the condition containing the complementary DNA chain S1 and Exo I, which was employed for FR detection in the later experiments after the optimization of various experimental parameters.

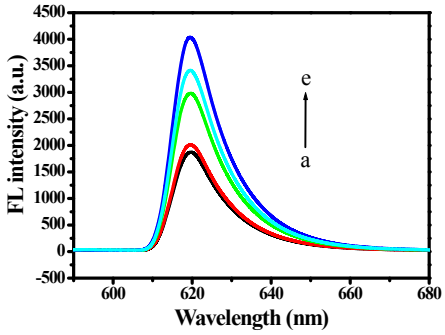

Fig.S5 Fluorescence emission spectra of different condition. (a) AgNCs-S2/SWCNTs. (b) AgNCs-S2/SWCNTs, FA-S1, and Exo I. (c) AgNCs-S2/SWCNTs, FA-S1, FR, and Exo I. (d) AgNCs-S2/SWCNTs and FA-S1. (e) AgNCs-S2.

6 Optimization of assay parameters based on visual analysis.

Visual analysis proposed here is an intuitive and concise analysis method after a long-term research and exploration.[9] With using nonlinear mathematical model [See below], the experiment results were calculated and drawn into 2.5 D images. Through the analysis of produced graphics, we can easily find the appropriate dosage of area of ideal index factors. It is a kind of accurate and reliable method for experimental analysis.[10]

$$y = b + \sum_{j=1}^{4}\left[w_j \frac{2}{1+e^{-2\left(\sum_{i}^{2} W_{ij} x_i + b_j\right)}} - 1 \right],$$

where x_i is the input value of model, y is the calculated value of model, w_{ij}, w_j, b_j, b are the parameters of model.

We designed 10 different condition of the mixture solution for FR detection and the results were filled on the right. According to the experimental results, the reasonable nonlinear mathematical model

was proposed and fitted experimental data obtained. Based on the experimental results and the model, visualization analysis figures were draw by using computer software[11] and we can deduce the optimized conditions from the figures obtained. As the same method described for pH optimization, Fig. S6 (concentration of Exo I as the abscissa, ordinate with the temperature, digestion time and pH value, respectively), Fig. S7 (temperature as the abscissa, ordinate with the concentration of Exo I, digestion time and pH value, respectively) and Fig. S8 (digestion time as the abscissa, ordinate with concentration of Exo I, temperature and pH value, respectively) were obtained.

No.	pH	Temperature (°C)	Concentration of Exo I (U)	Digestion Time (min)	Fluorescence intensity (a.u.)
1	4	32	110	9	2216
2	5	46	180	20	2354
3	6	55	50	7	2092
4	6.5	25	110	19	2986
5	7.5	33	180	6	2704
6	9	48	70	17	2342
7	9	59	130	3	1984
8	10	27	200	15	2408
9	12	41	90	1	1905
10	13	53	160	12	1923

pH=7, concentration of Exo I stood on 110 U, 25 °C as the incubation temperature and digestion kept for 20 min.

Table 1 Multifactor and multilevel Visual Design and experimental fluorescent results under the corresponding conditions.

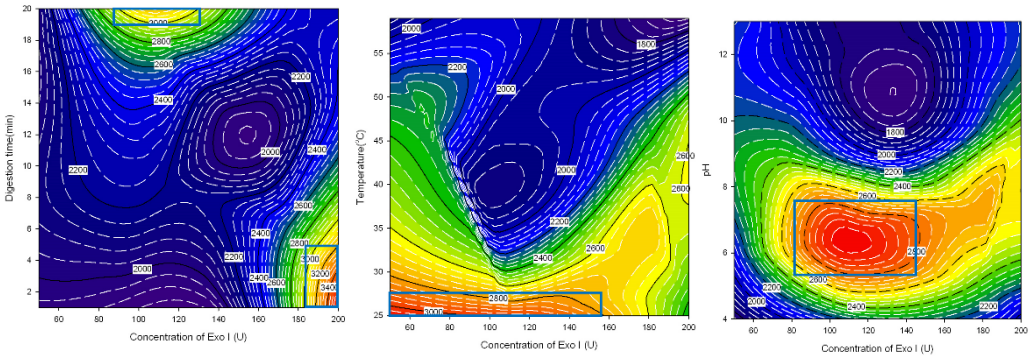

Fig. S6 Fluorescence intensity contour graph based on the concentration of Exo I in samples.

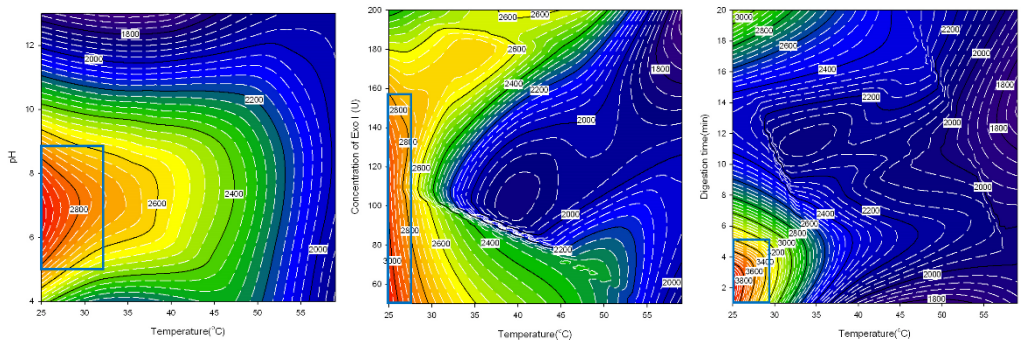

Fig. S7 Fluorescence intensity contour graph based on the temperature of samples.

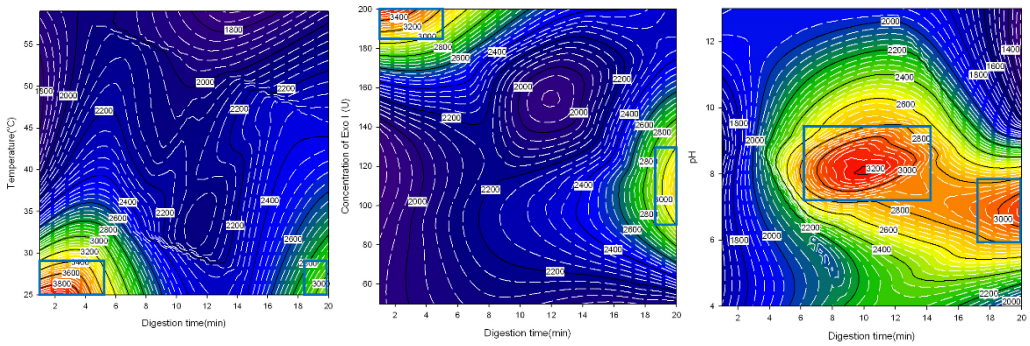

Fig. S8 Fluorescence intensity contour graph based on the digestion time of Exo I in samples.

7 Kinetic behaviors investigation.

Study of the kinetic behaviors of AgNCs-S2/SWCNTs was of great significance because it left a relationship with practical application. If the kinetic was very fast, the developmental prospects would be more fantastic and more attractive. Fig. S9 showed kinetic behaviors of AgNCs-S2/SWCNTs with various concentrations of FR in the presence of FA-S1 and 110 U Exo I. Fig. S9A showed its fluorescence reappearing as a function of incubation time. In the reaction solution containing 2 ng/mL FR, the fluorescent intensity exhibited a rapid rising in the first 10 min and a slow increasing over the last 5 min period. It was hypothesized that the surface effect between SWCNTs and AgNCs-S2 with a large conjugate plane was broken due to the formation of duplex DNA. FR-FA-S1/S2-AgNCs was desorbed and released from SWCNTs' surface automatically. In the presence of various concentrations of FR (0.1, 0.5, 1.0, 2.0 and 3.0 ng/mL), the corresponding results of fluorescence enhancement of AgNCs-S2/SWCNTs were consistent with that of 2 ng/mL as Fig. S9B showed. Up to now, we can conclude that the formation of duplex FR-FA-S1/S2-AgNCs reduced the absorbance of AgNCs-S2 on SWCNTs surface and the fluorescence quenching efficiency. Thus an overall fluorescence enhancement compared to that without the addition of FR was contributed. What's more, the kinetic behaviors presented that the incubation time was less than 20 min, which was much shorter than other published articles,[12] and of great significance when applied into real sample detections. The experimental results demonstrated that our proposed label-free "turn-on" fluorescent approach could be used as a sensitive approach for FR detection in aqueous solution.

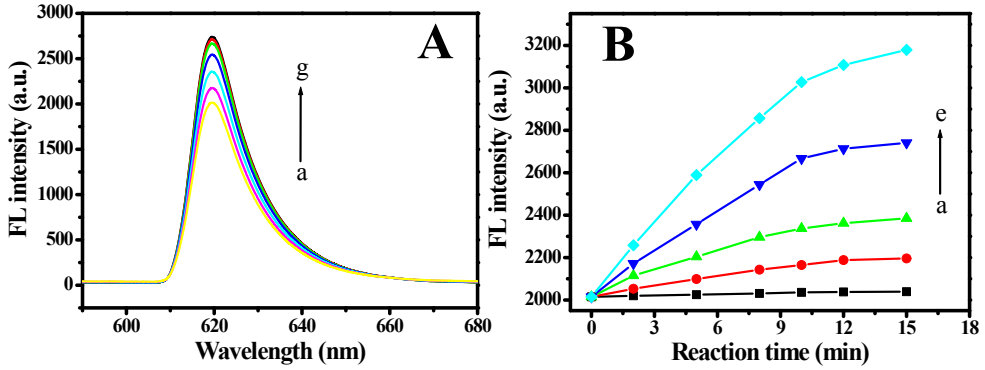

Fig. S9 (A) Fluorescence emission spectra representing our kinetic studies of the fluorescence enhancement of 2 ng/mL FR on AgNCs-S2/SWCNTs. (a-g): Fluorescence emission with scan times of 0, 2, 5, 8, 10, 12, 15 min. (B) Fluorescence intensity of AgNCs-S2/SWCNTs as a function of time in the presence of various concentrations of FR, (a-f): 0.1, 0.5, 1, 2 and 3 ng/mL.

8. Specificity and application of the biosensor.

The specificity of our proposed biosensor was investigated as below. The concentration of FR was set at 3.0 ng/mL, while the concentrations of the interfering substance were 3.0 μg/mL of CVH, 1.0 μg/mL of IgG, and 0.5 μg/mL of BHb and BSA. As shown in Fig. S10, the enhancement of fluorescence intensities in the presence of interfering substance was little, slight and negligible, and none of the tested metal ions gave fluorescence intensity higher than half of that produced by 3.0 ng/mL FR, suggesting that our proposed biosensor owned excellent specificity and good anti-interference ability. Such excellent selectivity was attributed to the specific affinity between FA and FR, and it ensured its great potential for further using.

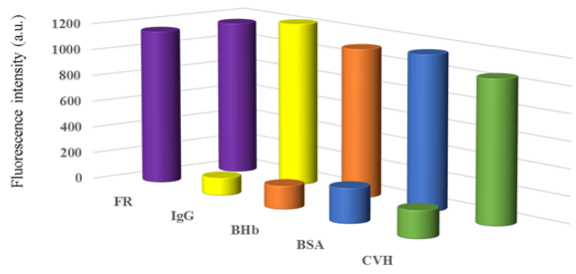

Fig. S10 (Front row) Effect of different competitive protein on the fluorescence emission of AgNCs-S2/SWCNTs compared with FR. (Back row) Interference study of FR by our fluorescent biosensor.

9 Comparison with other published biosensor.

Ref.	13	14	15	16	17	18	19	Ours
Selectivity	Good with 3	Excellent with	Good with 3	Good with 3	Good with 2	Good with 3	Good with 5	Good with 4

List	Sensitivity
A peptide nanotube–folic acid modified graphene electrode	8 nM
Self-Assembly of Folate onto polyethyleneimine-Coated CdS/ZnS	10 ng mL^{-1}
Small Molecule-Linked DNA based electrochemical sensor	0.19 ng/mL
Terminal protection and supersandwich DNAzyme amplification	0.3 ng/mL
A colorimetric sensor based on terminal protection-assisted cascade	0.46 ng/mL
Terminal protection of small molecule-linked ssDNA	0.03 nM
Electrochemiluminescence biosensor based on terminal protection of	0.1204 nmol/L
Silver nanoclusters based label-free fluorescent sensor	33 pg/mL

Table S2 Comparison with other published biosensor.

10 Relative uptake effciency of nanocomplexes by Hela cells

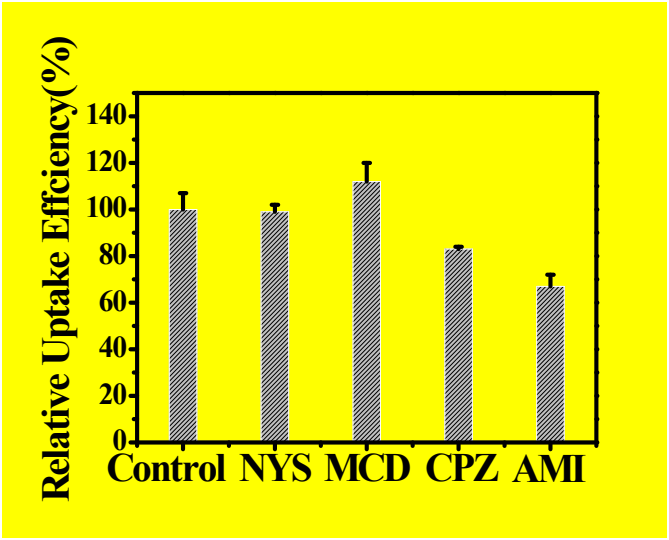

Fig. S11 Relative uptake effciency of nanocomplexes by Hela cells.

11 Fluorescent intensity of various numbers of Hela cells

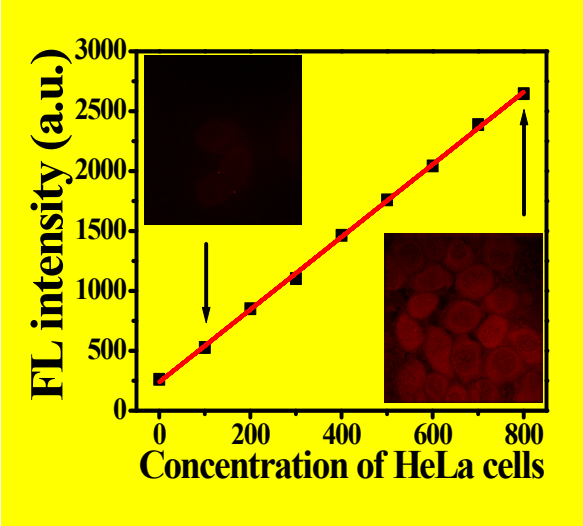

Fig. S12 Fluorescent intensity of various numbers of Hela cells. Inset: Two fluorescent images corresponding to 100, 700 mL^{-1} Hela cells.

References

1.(a) G. F. Wang, X. P. He, L.Wang, X. J. Zhang, *Biosens. Bioelectron.,* 2013, *42*, 337. (b) B. Sahoo, K. S. P. Devi, S. K. Sahu, S. Nayak, T. K. Maiti, D. Dhara, P. Pramanik, *Biomater. Sci.,* 2013, *1*, 647. (33) S. V. Lale, R. G. Aswathy, A. Aravind, D. S. Kumar, V. Koul, *Biomacromolecules.,* 2014, *15*, 1737.

2. (a) C. I. Richards, S. Choi, J. C. Hsiang, Y. Antoku, T. Vosch, A. Bongiorno, Y. L.Tzeng, R. M.Dickson, *J. Am. Chem. Soc.,* 2008, *130*, 5038. (b) B. Sengupta, C. M. Ritchie, J. G. Buckman, K. R.

Johnsen, P. M. Goodwin, J. T. Petty, *J. Phys. Chem. C.,* 2008, *112*, 18776.
3. A. Ono, S. Cao, H. Togashi, M. Tashiro, T, Fujimoto, T. Machinami, S. Oda, Y. Miyake, I.Okamoto, Y. Tanaka, *Chem. Commun.,* 2008, 4825.
4. R. Mo, T. Jiang, R. DiSanto, W. Tai, Z. Gu, *Nat. Commun*., 2014, 5, 3364.
5. R. H. Yang, J. Y. Jin, Y. Chen, N. Shao, H. Z. Kang, Z. Xiao, Z. W. Tang, Y. R. Wu, Z. Zhu, W. H. Tan, *J. Am. Chem. Soc.,* 2008, *130*, 8351.
6. J. Sharma, R. C. Rocha, M. L. Phipps, H. C. Yeh, K. A. Balatsky, D. M.Vu, A. P. Shreve, J. H. Werner, J. S. Martinez, *Nanoscale*., 2012, *4*, 4107.
7. (a) L. B. Zhang, L. Tao, B. L. Li, L. Jing, E. K. Wang, *Chem. Commun.,* 2010, *46*, 1476.
(b) P. J. Boul, D. G. Cho, G. M. A. Rahman, M. Marquez, Z. P. Ou, K. M. Kadish, D. M. Guldi, J. L. Sessler, *J. Am. Chem. Soc.,* 2007, *129*, 5683. (c) L. Zhang, R. Zhang, P. Cui, W. F. Cao, F. Gao, *Chem. Commun.,* 2013, *49*, 8102.
8. Y. Cao, S. Zhu, J. C. Yu, X. J. Zhu, Y. M. Yin, G. X. Li, *Anal. Chem.,* 2012, *84*, 4314.
9. W. Song, Y. Sun, L. Luo, *Applied Chemical Industry.,* 2008, *37*, 746.
10. (a) C. Yu, Y. Sun, J. Wang, F. Lu, D. Zhou, *NAT. PROD. RES .,* 2013, *3*, 600. (b) Y. Sun, W. Tao, G. Bian, *Food Science.,* 2011, 117.
11. Y. Sun, M. Zhong, X. Hu, C. Zhai, H. Chen, X. Zhang, *China synthetic resin and plastics.,* 2012, *29*, 18.
12.(a) X. J. Yang, Z. Q. Gao, *Nanoscale.,* 2014, *6*, 3055. (b) R. B. Li, C. M. Wang, Y. H. Hu, O. Zheng, L. H. Guo, Z. Y. Lin, B. Qiu, G. N. Chen, *Biosens. Bioelectron.,* 2014, *58*, 226.
13. J. J. Castillo, W. E. Svendsen, N. Rozlosnik, P. Escobar, F. Martineza, J. Castillo-Leon, *Analyst.,* 2013, *138*, 1026.
14. Y. Zhang, J. M. Liu, X. P. Yan, *Anal. Chem.,* 2013, *85*, 228.
15. Y. Cao, S. Zhu, J. C. Yu, X. J. Zhu, Y. M. Yin, G. X. Li, *Anal. Chem.,* 2012, *84*, 4314.
16. G. F. Wang, X. P. He, L. Wang, X. J. Zhang, *Biosens. Bioelectron.,* 2013, *42*, 337.
17. J. Zhao, S. S. Hu, X. X. Chen, B. Zhang, K. M. Wang, X. J. Liu, *SENSOR ACTUAT B-CHEM.,* 2014, *202*, 1243.
18. Y. Y. Xu, B. Y. Jiang, J. Q. Xie, Y. Xiang, R.Yuan, Y. Q. Chai, *Talanta.,* 2014, *128*, 237.
19. R. B. Li, C. M. Wang, Y. H. Hu, O. Zheng, L. H. Guo, Z. Y. Lin, B. Qiu, G. N. Chen, *Biosens. Bioelectron.,* 2014, *58*, 226.